

Angular Distribution of Neutrons Scattered by Helium*

ROBERT K. ADAIR

University of Wisconsin, Madison, Wisconsin

(Received December 28, 1951)

A proportional counter filled with helium was irradiated with monoenergetic fast neutrons produced by bombarding thin lithium and tritium-filled zirconium targets with protons from the electrostatic generator. Angular distributions of the neutrons scattered by helium were determined by measuring the distribution in energy of the pulses from recoiling alpha-particles with a differential discriminator. Measurements were made for eleven different neutron energies from 400 kev to 2730 kev. The angular distributions were consistent with a description of the neutron-helium interaction in terms of an inverted $P_{3/2}-P_{1/2}$ doublet in He^5 , split by about 5 Mev.

I. INTRODUCTION

AN examination of the interaction of neutrons and protons with alpha-particles can provide information on the virtual ground states of He^5 and Li^5 . According to the quasi-atomic model of nuclei the lowest state of He^5 or Li^5 should be a 2P state. The sign and magnitude of the splitting in energy of the $P_{3/2}$ and $P_{1/2}$ components of the doublet is of particular interest since the characteristics of the splitting may be related to specific nucleon-nucleon spin orbit forces.

Measurements of the $n-\alpha$ back-scattering cross section by Staub and Tatel¹ showed some indication of a doublet structure near 1-Mev neutron energy. These authors interpreted their results in terms of a form of dispersion theory introduced by Bloch² and concluded their data could be fitted by either a regular or inverted $P_{3/2}-P_{1/2}$ doublet split by about 300 kev. However, Wheeler and Barschall³ showed that the $n-\alpha$ angular distribution measurements of Barschall and Kanner⁴ at a neutron energy of 2.4 Mev indicated a much stronger spin orbit coupling than could be expected from the level assignments of Staub and Tatel. Hall and Koontz⁵ measured the $n-\alpha$ angular distribution and total cross section at neutron energies from 0.6 to 1.8 Mev. They attempted to analyze their data in terms of a close doublet but did not succeed in obtaining a fit to their measurements. The presence of the low energy group of neutrons from the $\text{Li}(p,n)$ reaction affected their results adversely.⁶

From an analysis of more quantitatively reliable data on the $p-\alpha$ differential cross section and the $n-\alpha$ total cross section it was concluded that an inverted $P_{3/2}-P_{1/2}$ doublet is formed in He^5 and Li^5 with a splitting of the order of 5 Mev.⁷ In view of the uncertainties in the angular distribution measurements and their usefulness in corroborating the level assignments, it seemed

desirable to make further measurements of these distributions.

II. EXPERIMENTAL PROCEDURE

Monoenergetic neutrons were used to bombard helium in a proportional counter, and the angular distribution of the scattered neutrons was determined by measuring the distribution in energy of the helium recoils. Barschall⁴ has pointed out that the distribution in energy of the alpha-particle recoils in the laboratory system is proportional to the differential scattering cross section per unit solid angle as a function of $\cos\vartheta$, where ϑ is the angle of scattering in the center-of-mass system. Therefore, the distribution of pulses from the counter represents the differential scattering cross section as a function of the cosine of the scattering angle.

Figure 1 shows the proportional counter used in these measurements. The most important difference between this counter and that described by Koontz and Hall⁸ is the utilization of guard sleeves held at an intermediate potential. An important limitation on the use of proportional counters with gas amplification is the reduction of the gas multiplication near the ends of the counter caused by distortion of the field by wire supports and guard sleeves held at the potential of the wire. An attempt was made to reduce this effect by using guard sleeves held at an intermediate potential.⁹ The sleeves used on this counter consisted of ceramic tubing which had an outside diameter of 0.040 inch and an inside diameter of 0.010 inch. The outside surface was coated with Aquadag to provide a conducting surface, and held at an appropriate intermediate potential. Since the dielectric constant of the ceramic was about four, it was necessary to coat the inside of the ceramic, which was in contact with the wire, to preclude the production of excessive fields in small gaps between the ceramic and wire. Such fields could cause small gas breakdowns.

The chamber was used in conjunction with a Model 100 amplifier and preamplifier. The rise time of the amplifier was 0.5 microsecond and the clipping time 32 microseconds. Pulse-height distributions were

* Work supported by the AEC and the Wisconsin Alumni Research Foundation.

¹ H. Staub and H. Tatel, Phys. Rev. **57**, 936 (1940).

² F. Bloch, Phys. Rev. **58**, 829 (1940).

³ J. Wheeler and H. H. Barschall, Phys. Rev. **58**, 682 (1940).

⁴ H. H. Barschall and M. H. Kanner, Phys. Rev. **58**, 590 (1940).

⁵ T. A. Hall and P. G. Koontz, Phys. Rev. **72**, 196 (1947).

⁶ T. A. Hall, Phys. Rev. **72**, 196 (1947).

⁷ R. K. Adair, Phys. Rev. **82**, 750 (1951).

⁸ P. G. Koontz and T. A. Hall, Rev. Sci. Instr. **18**, 643 (1947).

⁹ A. L. Cockroft and S. C. Curran, Rev. Sci. Instr. **22**, 37 (1951).

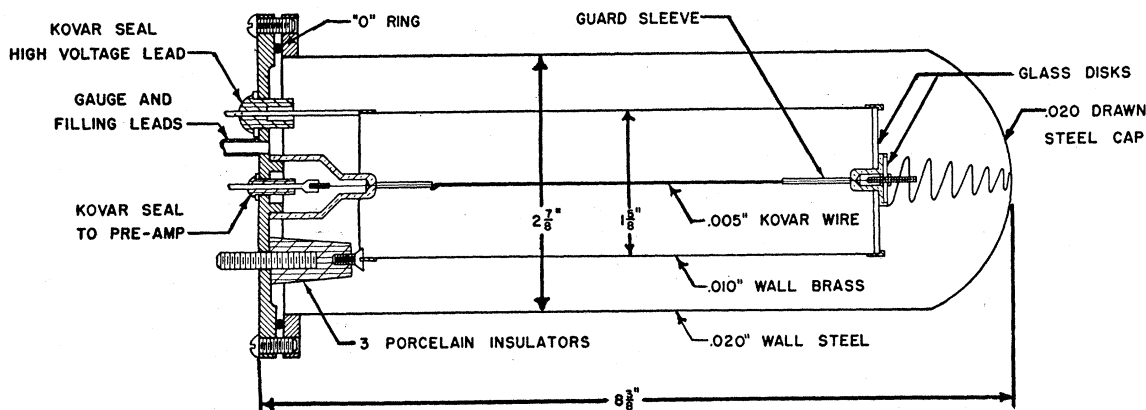


FIG. 1. Proportional counter.

measured with a single channel differential discriminator. A channel width of $1\frac{1}{2}$ volts, held constant by a dry cell, was used. The position of the bottom of the channel could be varied from 0 to 50 volts.

The energy resolution of the counter was checked by measuring the pulse-height distribution from the nitrogen (n, p) reaction when nitrogen was introduced into the counter, and by measuring the pulse distributions of the α -particles from a polonium source on the counter wall. In both cases the pulse distributions had a width at half-maximum of about five percent of the pulse energy.

Measurements of the n - α angular distribution were made at neutron energies of 1000 kev, 1200 kev, 1400 kev, 1700 kev, 2000 kev, 2400 kev, and 2730 kev by irradiating the counter with fast neutrons from the $T(p, n)$ reaction. The tritium was absorbed in a zirconium film which had been evaporated onto a wolfram backing. Two-Mev protons lost about 30-kev energy in passing through this target. Monoenergetic neutrons of the required energies were produced by bombarding the target with protons accelerated by the electrostatic generator. It is in this region above 1 Mev that the results of Hall and Koontz were obscured by the low energy group of neutrons from the $Li(p, n)$ reaction which they used. For the present measurements the counter was filled with $1\frac{1}{2}$ atmospheres of argon, $1\frac{1}{2}$ atmospheres of helium, and 1.4 cm of CO_2 . With this filling, the most energetic alpha-particle recoils from the highest neutron energy used had a range of about 7 mm. The CO_2 was added to reduce the rise time of the pulses from about 50 microseconds to about 5 microseconds. Since the clipping time was 32 microseconds, the maximum height of the pulse was not sensitive to the small variations in pulse rise time which are caused by differences in electron collection time from different recoil tracks. The counter was placed in position so that the axis of the counting volume was aligned with the direction of the proton beam, the center of the counting volume being about 4 inches from the target. A gas multiplication of about 15 was obtained with

2000 volts between the center wire and the wall and 400 volts between the wire and sleeve. The potential was supplied by dry cells. Pulse-height distributions were obtained by recording the number of counts which fell into the discriminator channel as a function of the bias of the channel. The neutron flux was monitored indirectly by measuring the proton current incident on the target. The crosses on Figs. 4, 5, and 6 represent the distributions obtained in this way; the ordinate of each point is proportional to the number of counts in the channel per unit neutron flux; the abscissa is proportional to the bias voltage measured to the center of the channel.

Slightly different procedures were used to obtain the angular distributions at energies of 400 kev, 600 kev, 750 kev, and 865 kev. Since the low energy group of neutrons from the $Li(p, n)$ reaction does not seriously interfere with the measurements at these energies, it seemed advantageous to make use of the larger neutron flux available from the $Li(p, n)$ reaction. The counter was again placed in line with the proton beam, but with the center of the counting volume 7 inches from the target. For these measurements the counter was filled with 3 atmospheres of helium and 2.4 cm of CO_2 . A gas multiplication of about 15 was produced with 1200 volts between the wall and wire. The crosses on Figs. 2 and 3 show the distributions obtained in this fashion.

III. EXPERIMENTAL RESULTS

Corrections must be applied to the pulse-height distribution before one can relate them to differential cross sections. In particular, allowance must be made for tracks which enter or leave the active volume expending only part of their energy in this volume. Effects produced by the distortion of the field near the guard sleeves are also important. Measurements reported by Rossi and Staub¹⁰ show that under unfavorable conditions the reduction in field near a wire support of larger diameter than the wire will produce a region of reduced

¹⁰ B. Rossi and H. Staub, *Ionization Chambers and Counters* (McGraw-Hill Book Company, Inc., New York, 1949).

gas multiplication which may extend as much as a cm from the support. In the counter used in the present experiment the inside of the guard sleeve is held at the potential of the wire. Since the inside diameter of the sleeve is twice the size of the wire, distortion will occur. However, the field variation is much smaller than in the example presented by Rossi and Staub, and the gas multiplication is less sensitive to the field. The extent of this region was then estimated rather arbitrarily as 4 mm.

The fraction of the pulses of energy ϵ which were reduced in energy was calculated and added to channel ϵ . This addition represents pulses which fell into lower channels and must therefore be subtracted from these channels. The distribution from the lower channels will depend upon the spectrum of energies of the degraded pulses. Pulses lost to a channel by the wall effect would have a spectrum of energies such as to distribute them evenly among the lower channels if the ionization density along the track were constant. The correction to the distribution was made by assuming all of the degraded pulses including those which were reduced in energy by the end effect would have a distribution such that the counts added to channel ϵ were contributed

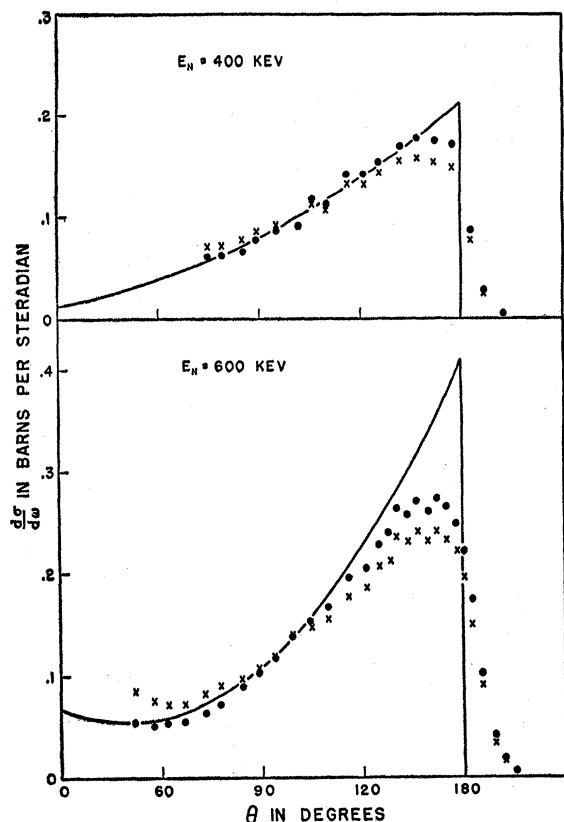


FIG. 2. Angular distribution in the center-of-mass system of neutrons scattered by helium at neutron bombardment energies of 400 kev and 600 kev. The crosses represent the uncorrected data. The solid circles represent the data corrected for end effects and wall effects. The solid curve shows the distribution calculated from Eqs. (1) and (4).

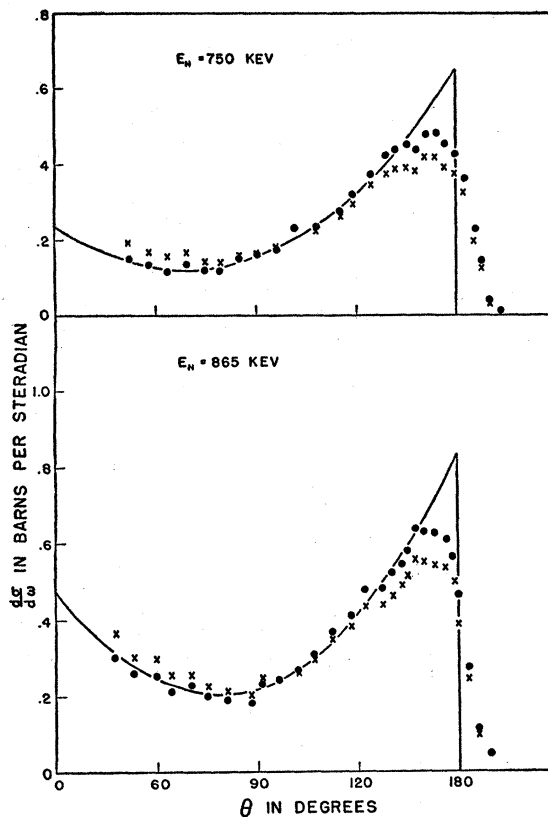


FIG. 3. Angular distribution in the center-of-mass system of neutrons scattered by helium at neutron bombardment energies of 750 kev and 865 kev. The crosses represent the uncorrected data. The solid circles represent the data corrected for end effects and wall effects. The solid curve shows the distribution calculated from Eqs. (1) and (4).

equally by the lower channels. This contribution was therefore subtracted from the lower channels. The lack of knowledge of the behavior of the gas multiplication at the ends of the counter makes a more detailed study of the correction seem unprofitable. A correction was also applied for the recoils caused by collisions of the neutrons with the carbon and oxygen from the CO_2 . The uncertainty in the whole correction is estimated to be about one-half the value of the correction and is larger than the purely statistical errors. The distribution curve is, of course, affected by the energy resolution of the counter. The uncertainty in this resolution is so large that it seemed best not to attempt such a correction.

The solid circles on Figs. 2-6 represent the corrected distributions. When allowance is made for the effect of the low energy group of neutrons in the measurements of Hall and Koontz,⁵ the present results are in good agreement with theirs over the energies which they measured. The agreement of the distributions with those of Barschall and Kanner at 2.4 Mev and the measurements of Huber¹¹ at neutron energies of 0.52, 0.7, 1.91, 2, 2.5, and 2.6 Mev is quite good.

¹¹ P. Huber (private communication).

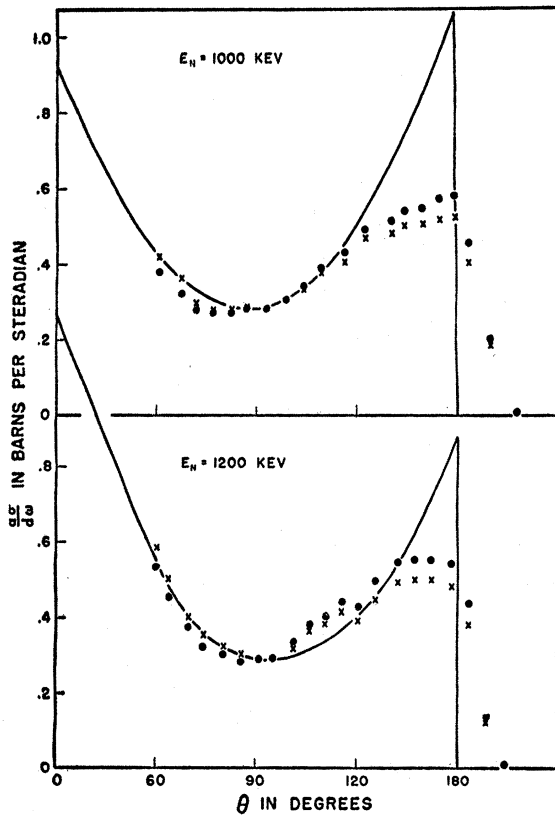


FIG. 4. Angular distribution in the center-of-mass system of neutrons scattered by helium at neutron bombardment energies of 1000 kev and 1200 kev. The crosses represent the uncorrected data. The solid circles represent the data corrected for end effects and wall effects. The solid curve shows the distribution calculated from Eqs. (1) and (4).

IV. INTERPRETATION

When coupling between spin and orbital angular momentum is taken into account, the differential scattering cross section for a neutron scattered by a nucleus of spin zero can be written,

$$d\sigma/d\Omega = k^{-2} |e^{i\delta_0} \sin\delta_0 + \cos\vartheta (2e^{i\delta_+} \sin\delta_+ + e^{i\delta_-} \sin\delta_-)|^2 + k^{-2} |\sin\vartheta (e^{i\delta_-} \sin\delta_- - e^{i\delta_+} \sin\delta_+)|^2, \quad (1)$$

where k is the wave number of the neutron, δ_0 is the s -wave phase shift, and δ_+ and δ_- are the phase shifts for the $P_{3/2}$ - and $P_{1/2}$ -waves, respectively. The interaction of waves associated with an angular momentum greater than one will be neglected at the energies of interest here. Since Eq. (1) is a second-order equation in $\cos\vartheta$, the pulse-height distributions should take the form of parabolas. The three coefficients determining the parabola are completely specified at any energy by the measured angular distributions and the total cross section. Although one can then solve for the three unknown phase shifts, the experimental uncertainties in the distribution measurements are large and it appears more useful to use them in a corroborative

manner, comparing them with differential cross sections estimated from other considerations.

Nuclear reactions in general are conveniently discussed in terms of the wave function at the nuclear surface. According to Wigner and Eisenbud¹² one can set up Hermitian boundary conditions on the nuclear surface which determine a complete set of eigenfunctions. The scattering matrix can then be expressed in terms of the values of the eigenfunctions on the nuclear surface and their characteristic energies. The choice of boundary conditions is somewhat arbitrary. A convenient choice is,

$$\varphi = (d \ln r \chi / d \ln r)_{r=a} = -l, \quad (2)$$

where χ is the normalized internal wave function and a is the nuclear radius. A function R may be defined which is equal to $a/(\varphi+l)$. For elastic scattering R can be expanded in a series $R = \sum \gamma_\lambda^2 / (E_\lambda - E)$, where the E_λ are characteristic energies associated with the eigenfunctions χ_λ determined by the nuclear Hamiltonian and the boundary conditions of Eq. (2) and $\gamma_\lambda = (\hbar^2/2m)^{1/2} \times \int \chi_\lambda V dS$, where V is the exterior radial wave func-

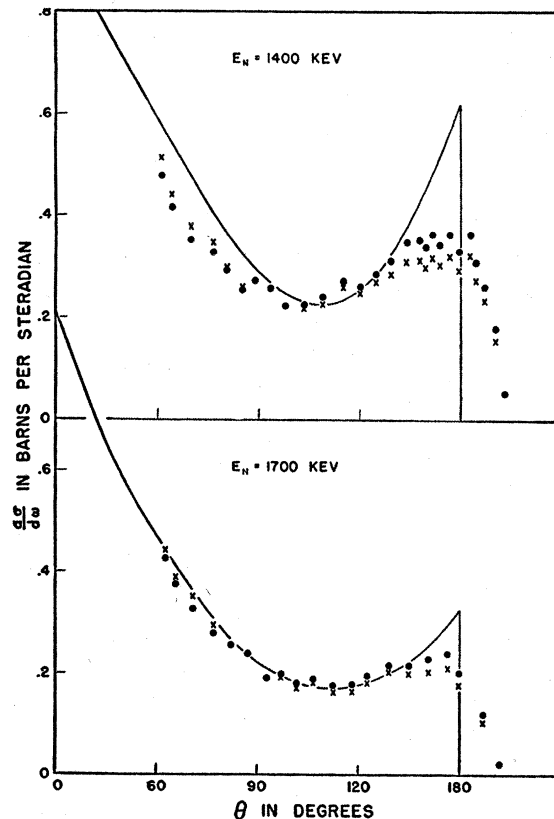


FIG. 5. Angular distribution in the center-of-mass system of neutrons scattered by helium at neutron bombardment energies of 1400 kev and 1700 kev. The crosses represent the uncorrected data. The solid circles represent the data corrected for end effects and wall effects. The solid curve shows the distribution calculated from Eqs. (1) and (4).

¹² E. P. Wigner and L. Eisenbud, Phys. Rev. 72, 29 (1947).

tion of the two particles normalized over the nuclear surface.

When the only reaction which can occur is elastic scattering, the S -matrix is defined uniquely by the scattering phase shifts, $S_{l,j} = \exp(2i\delta_{l,j})$. We can express δ in terms of the logarithmic derivative, φ ,

$$\delta = -\tan^{-1}[(\varphi F - aF')/(\varphi G - aG')],$$

where F and G are the regular and irregular free particle wave functions¹³ evaluated at a and the prime indicates the derivative with respect to r . Using $R_{l,j} = a/(\varphi_{l,j} + l)$ we can write

$$\delta = \tan^{-1} \frac{ka/(F^2 + G^2)}{(a/R) - d \ln(F^2 + G^2)/d \ln(ka) - l} - \tan^{-1} \frac{F}{G}. \quad (3)$$

When E is near E_λ , we can approximate R by one term in the expansion and obtain the single level Breit-Wigner formula

$$\delta = \tan^{-1} \frac{k\gamma^2/(F^2 + G^2)}{E_\lambda - E + \Delta} - \tan^{-1} \frac{F}{G}, \quad (4)$$

where

$$\Delta = -\frac{\gamma^2}{a} \left(\frac{d \ln(F^2 + G^2)}{d \ln ka} + l \right).$$

In general, a resonance energy, E_r , can be defined in different ways. A convenient definition is $E_r = E_\lambda + \Delta$. This will not, in general, be the energy at which the scattering cross section is a maximum, but it will be very near the energy at which the reaction particles have the highest probability of forming a compound state. Since the variation of the phase shift, and hence the cross section, will be large near resonance, the most reliable and easily interpreted experimental measurements are made near resonance. The level shift, Δ , represents the difference between the energies associated with the boundary condition and that which results in a resonance in the reaction. In order that R can be adequately represented by one term in the series at energies near resonance, the shift Δ should be much smaller than γ^2/a . It is then important to choose boundary conditions which will result in a small level shift. The boundary condition given in Eq. (2) was chosen to insure an adequately small level shift in the examples considered here.

Critchfield and Dodder¹⁴ have shown that the $p-\alpha$ differential cross-section measurements of Freier *et al.*¹⁵ are consistent with two sets of phase shifts, one representing an inverted doublet with an undetermined large splitting, the other corresponds to a regular doublet with a splitting of about one Mev. Measurements of the

¹³ These functions were computed with the aid of tables prepared by Bloch, Hull, Broyles, Bourcius, Freeman, and Breit, *Revs. Modern Phys.* **23**, 147 (1951).

¹⁴ C. L. Critchfield and D. C. Dodder, *Phys. Rev.* **76**, 602 (1949).

¹⁵ Freier, Lampi, Sleator, and Williams, *Phys. Rev.* **75**, 1345 (1949).

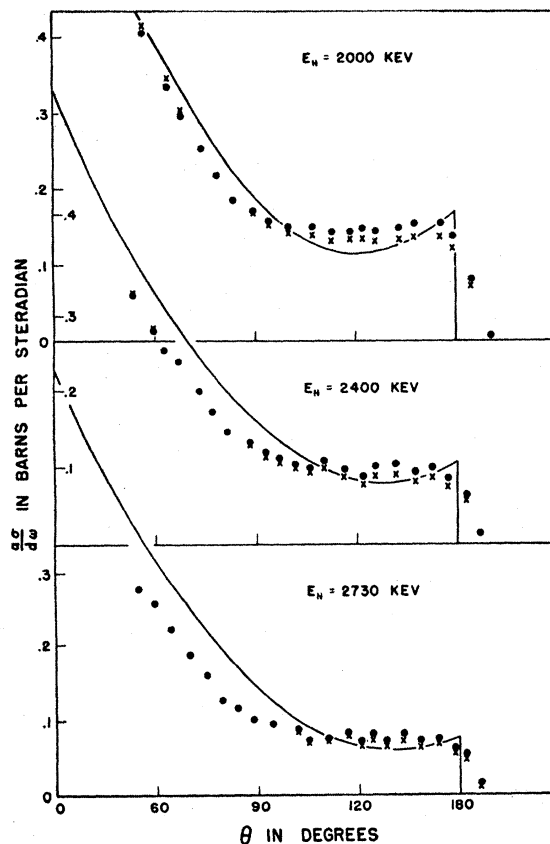


FIG. 6. Angular distribution in the center-of-mass system of neutrons scattered by helium at neutron bombardment energies of 2000 kev, 2400 kev, and 2730 kev.

polarization of the scattered protons¹⁶ show that the former alternative is correct. The points on Fig. 7 represent Critchfield and Dodder's values of the phase shifts for the inverted doublet together with their estimate of the probable error. The curves represent the best fit to the points obtained by trial and error from Eq. (4). Corresponding values of the parameters were $a = 2.9 \times 10^{-13}$ cm, $\gamma^2(P_{3/2}) = \gamma^2(P_{1/2}) = 17.6 \times 10^{-13}$ Mev cm, $E_\lambda(P_{3/2}) = 3.65$ Mev, and the doublet splitting $E_\lambda(P_{3/2}) - E_\lambda(P_{1/2}) = 5$ Mev. It is clear that the parameters for the $P_{3/2}$ level are somewhat arbitrary. The s -wave curve was computed using $R_s = 0$. A small negative value of R_s , as might be expected from the contributions of high-lying levels, would improve the fit.

The total $n-\alpha$ cross section will equal

$$\sigma = 2\pi k^{-2} \sum_{l,j} (2j+1) \sin^2 \delta_{l,j}, \quad (5)$$

where $\delta(P_{3/2})$ and $\delta(P_{1/2})$ are calculated from Eq. (4). The points on Fig. 8 are the experimental values of Bashkin *et al.*,¹⁷ while the solid curve represents the fit of Eq. (5) to the data, using the values of the parameters a , γ^2 , and the doublet splitting deduced from the $p-\alpha$ analysis. The discrepancy between the data and the

¹⁶ M. Heusinkveld and George Freier, *Phys. Rev.* **85**, 80 (1952).

¹⁷ Bashkin, Mooring, and Petree, *Phys. Rev.* **82**, 378 (1951).

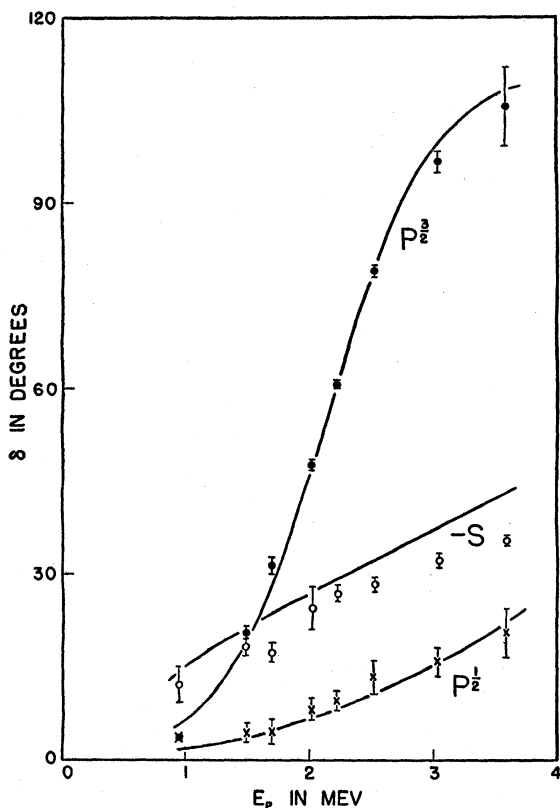


FIG. 7. Phase shifts for p - α scattering as a function of proton bombardment energy. The points represent the results of the analysis of Critchfield and Dodder, the solid curves show the phase shifts calculated from Eq. (4).

curve at 1.2 Mev is qualitatively accounted for by the lack of homogeneity in energy of the neutrons from the $\text{Li}(p,n)$ reaction which were used in the measurement of the total cross section. The effect of the low energy group of neutrons from this reaction reduces the experimental cross section. The He^5 levels are 1.25 Mev lower than the Li^5 levels, a shift attributable quantitatively to the difference in Coulomb energy. The n - α S -wave phase shifts were calculated by requiring the wave function to have the same logarithmic derivative at the nuclear surface as the p - α S -wave.

It seems reasonable to assume that the influence of higher angular momentum phase shifts is small. Critchfield and Dodder found no evidence for their presence in the analysis of the p - α scattering data. Since a/λ is only about one at 4 Mev, the penetration factor of neutrons with two units of orbital angular momentum will be of the order of five percent and one might expect D -wave phase shifts of a few degrees. The presence of such a D -wave phase shift will then affect the angular distribution at energies over 3 Mev through interference with the S - and P -waves. Since waves of different angular momentum do not interfere in total cross section the effect of D -waves on the total cross section should be negligible.

The description of the n - α interaction in terms of an inverted $P_{3/2}$ - $P_{1/2}$ doublet in He^5 , split by about 5 Mev, is in qualitative agreement with the n -angular distribution measurements. The solid curves on Figs. 2-6 show the differential cross sections calculated from Eq. (5) using the parameters derived from the analysis of the p - α differential cross section and the n - α total cross section data. The experimental distributions are roughly normalized to facilitate comparison with the theoretical differential cross sections. When the poor angular resolution and the rather large general uncertainties of the measurements are considered, their agreement with the curves seems satisfactory. A slightly smaller splitting and a lower value of $E_\lambda(P_{3/2})$ would result in a somewhat better fit, but the measurements are not sufficiently reliable to justify such a conclusion.

The angular distribution data of Huber *et al.* at energies over 3 Mev are not adequately represented by the phase shifts of Eq. (2). It appears to me, however, that these data may be fitted by reasonably small changes in these phase shifts and are not inconsistent with the general conclusions of the analysis.

DISCUSSION

The doublet splitting in He^5 has also been investigated by measuring the energy spectrum¹⁸ of neutrons produced in the bombardment of tritons by tritons. Two groups of neutrons were noted corresponding to the formation of broad states in He^5 , unbound by about 0.9 Mev and 3.5 Mev, respectively. A similar investigation has been made of the doublet splitting in Li^5 . Titterton and Brinkley¹⁹ observed the breakup of Li^5 produced by the $\text{Li}^5(\gamma,n)$ reaction and found evidence that Li^5 is produced in its lowest state and in a state

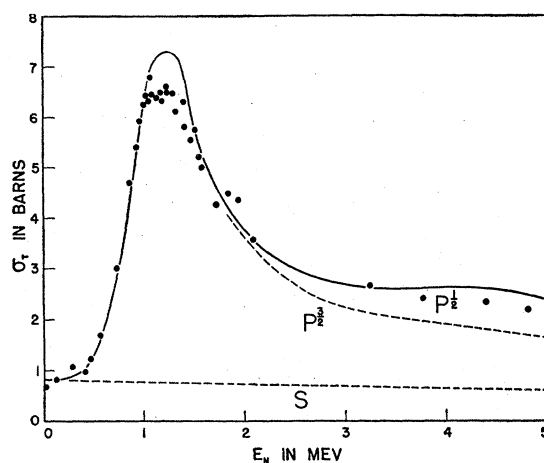


FIG. 8. n - α total cross section as a function of neutron bombardment energy. The points represent the experimental data of Bashkin *et al.* while the solid curve shows the cross section calculated from Eqs. (4) and (5). The dotted lines separate the contributions of the various partial cross sections.

¹⁸ W. J. Leland and H. M. Agnew, Phys. Rev. 82, 558 (1951).

¹⁹ W. E. Titterton and T. A. Brinkley, Proc. Roy. Soc. (London) A64, 202 (1951).

about 2.5 Mev higher. A complete description of these processes would require a more detailed knowledge of nuclear mechanics than is available, but as a first approximation it might be expected that the nucleus He^5 or Li^5 would be preferentially produced at the energy at which the extra nucleon has the highest probability of being found in the field of the alpha-particle. This energy will be near E_r , where $E_r = E_\lambda + \Delta$. For He^5 , $E_r(P_{3/2}) \approx 0.95$ Mev and $E_r(P_{1/2}) \approx 4$ Mev. For Li^5 , $E_r(P_{3/2}) \approx 2.1$ Mev and $E_r(P_{1/2}) \approx 5.3$ Mev. The splittings in E_r are smaller than the splittings in E_λ because of the change in Δ with energy. Considering the approximations made, the splittings in E_r of about 3 Mev are in satisfactory agreement with the experimental values obtained from the analysis of reaction products.

The difference between the resonance energy splitting of about 3 Mev and the characteristic energy splitting of about 5 Mev is dependent upon the value of the derivative of the wave function at the nuclear surface.²⁰ This value is sensitive to the choice of nuclear radius. A radius larger than the rather small value of 2.9×10^{-13} cm, determined from the shape of the $P_{3/2}$ resonances and the magnitude of the Coulomb energy shift between the He^5 and Li^5 states, would result in a smaller difference between the two splittings. However, the value of the characteristic energy difference, $E_\lambda(P_{3/2}) - E_\lambda(P_{1/2})$, must in any case be larger than the resonance energy splitting of about 2.7 Mev found from the reaction data, and probably lies between 4 and 5 Mev.

Since the E_λ are energies characteristic of the nuclear Hamiltonian and boundary conditions at the nuclear surface, the splitting, $E_\lambda(P_{3/2}) - E_\lambda(P_{1/2})$, can be regarded as the spin-orbit interaction energy averaged over the nuclear volume. Feingold and Wigner²¹ have estimated the splitting which might be expected from tensor forces. They find that this splitting, which occurs only in the second order of perturbation theory, can be only a few hundred kev. The ordinary relativistic Thomas splitting will be of the order of 50 kev.

According to Rosenfeld²² the Møller-Rosenfeld mixed-meson theory may lead to splittings of about M/m times the Thomas splitting, where M is the nucleon mass and m is the meson mass. This would still be an order of magnitude too small. Blanchard and Avery²³ have investigated the effect of specific nucleon-nucleon, ($\mathbf{L} \cdot \mathbf{S}$), spin-orbit forces on the splitting of the energy levels of a single particle outside of a closed shell. They find that if the strength of this velocity dependent interaction is comparable to that usually assumed for the static forces, then splittings of the necessary order of magnitude might be expected. Strong spin-orbit forces

²⁰ The importance of this effect has been discussed by J. Ehrman [Phys. Rev. **81**, 412 (1951)] and R. G. Thomas [Phys. Rev. **80**, 136 (1950)] with particular regard to the energy levels of C^{13} and N^{13} .

²¹ E. P. Wigner, private communication.

²² L. Rosenfeld, *Nuclear Forces* (Interscience Publishers, Inc., New York, 1949).

²³ C. H. Blanchard and R. Avery, Phys. Rev. **81**, 1067 (1951).

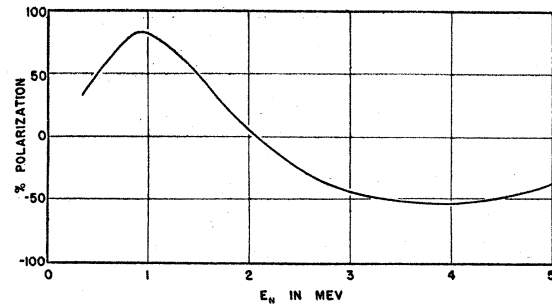


FIG. 9. Neutron polarization as a function of incident neutron energy of neutrons scattered by α -particles through 90° in the center-of-mass system.

have been used by Mayer²⁴ and Haxel *et al.*,²⁵ to explain certain characteristics of heavy nuclei. Low excited states of light nuclei also provide evidence²⁶ for strong spin-orbit forces.

Calculations such as those of Blanchard and Avery assume that the interaction can be represented adequately by the model of a single particle moving in the average potential of the closed shell core, and that the nucleon-meson coupling is sufficiently weak so that many-body forces can be neglected. The value obtained for the reduced width, γ^2 , characteristic of the $n-\alpha$ and $p-\alpha$ scattering is approximately equal to \hbar^2/Ma , where M is the reduced mass of the system. With this value of γ^2 and for $|E - E_\lambda| < \gamma^2/a$, Eq. (4) takes the same form as the result for scattering by a square well of depth E' , where $(E' + E) = \pi^2(l+1)^2\hbar^2/8Ma^2 = 37$ Mev, indicating that the interaction and the model of a nucleon moving in the average field of the alpha-particle may be a reasonably good approximation.

Schwinger²⁷ has pointed out that the strong spin orbit forces observed in the $n-\alpha$ interaction should result in a polarization of the scattered neutrons. The percent polarization in the X direction will equal

$$100 \frac{\bar{\sigma}_x}{d\sigma/d\Omega} = 100P, \quad (6)$$

where $\bar{\sigma}_x$ is the expectation value for the spin in the X direction and $d\sigma/d\Omega$ is the differential scattering cross section. For neutrons scattered out of an unpolarized beam

$$\bar{\sigma}_x = 2k^{-2} [\sin\varphi \sin\vartheta \{ \sin\delta_0 \sin\delta_- \sin(\delta_0 - \delta_-) - \sin\delta_0 \sin\delta_+ \sin(\delta_+ - \delta_0) \} + \sin\varphi \cos\vartheta \{ 3 \sin\delta_+ \sin\delta_- \sin(\delta_- - \delta_+) \}], \quad (7)$$

where only S - and P -waves are considered.²⁸

²⁴ M. G. Mayer, Phys. Rev. **75**, 1969 (1949).

²⁵ Haxel, Jensen, and Suess, Phys. Rev. **75**, 1766 (1949).

²⁶ Koester, Jackson, and Adair, Phys. Rev. **83**, 1250 (1951).

²⁷ J. S. Schwinger, Phys. Rev. **69**, 681 (1946).

²⁸ The calculational procedure is similar to that used by Wolfenstein in his analysis of reactions involving polarized protons. L. Wolfenstein, Phys. Rev. **75**, 1664 (1949).

Figure 9 shows the polarization of neutrons scattered from helium in the direction $\varphi = \vartheta = 90^\circ$, as a function of incident neutron energy. Polarizations were calculated from Eq. (6) and Eq. (7) using the phase shifts which described the $n-\alpha$ total cross section and the angular distribution. These polarizations should be quantitatively reliable below 2 Mev. At higher energies the uncertainties in the phase shifts and the influence of D -waves make the results of only qualitative value.

It may also be possible to use helium to analyze the polarization of fast neutrons, since the scattering of a polarized beam of neutrons from helium will show a left right asymmetry equal to $(1+P'P)/(1-P'P)$, where P' is the polarization of the incoming beam.

I wish to thank Professor H. H. Barschall for his advice on the experimental techniques involved in this work. I also wish to express my appreciation to Professor P. Huber for discussion of his measurements.

The Isotope Effect in Superconductivity. II. Tin and Lead*

B. SERIN, C. A. REYNOLDS, AND C. LOHMAN†

Physics Department, Rutgers University, New Brunswick, New Jersey

(Received December 13, 1951)

The critical magnetic fields, H , of various isotopic mixtures of tin and of lead have been measured as a function of temperature, T .

For tin, the critical temperature T_c at zero field, is related to the average mass number, M , by the relation $M^{0.46}T_c = \text{const}$. The critical magnetic fields, H_0 , at absolute zero are proportional to the critical temperatures. The normalized values of critical field, H/H_0 , are the same function of the variable T/T_c for all the isotopes. An analytic expression for this function giving the best fit to the experimental data is given.

The measurements on lead were made in the temperature range 1.6°K to 4.2°K. The data clearly indicate that the isotope effect is present in this superconductor.

1. INTRODUCTION

THIS investigation was a continuation of our work on the dependence of superconducting properties on isotopic mass which was originally discovered in mercury. The details of experimental technique and a bibliography are contained in our first paper,¹ which will be referred to as I. The present work was briefly reported at low temperature conferences² and is in

TABLE I. Critical field data for tin. The critical temperatures T_c , the critical fields at 0°K, H_0 , and the slope of the critical field-temperature curves at T_c , $(dH/dT)_{T_c}$, are tabulated as a function of the average mass number, M . The purities and H_0/T_c are also listed.

M	Purity (% Sn)	T_c (°K)	H_0 (oersteds)	H_0/T_c	$(dH/dT)_{T_c}$ (oersteds/ °K)
113.6	99.50	3.805	312	82.0	145
118.7	99.995	3.752	304	81.5	144
123.8	99.76	3.659	298	81.4	144

* This work has been supported by the joint program of the ONR and AEC, the Rutgers University Research Council, and the Radio Corporation of America.

† The parts of this paper dealing with the measurements on lead are based on an M.S. thesis submitted by C. Lohman to the Graduate Faculty of Rutgers University.

¹ Reynolds, Serin, and Nesbitt, *Phys. Rev.* **84**, 691 (1951).

² Serin, Reynolds, and Nesbitt, *Proceedings of the Low Temperature Symposium* (National Bureau of Standards, March 27 to 29, 1951); C. A. Reynolds and B. Serin, *Proceedings of the International Conference on Low Temperature Physics* (Oxford, England, August 22 to 28, 1951).

general agreement with the work of Lock, Pippard, Shoenberg,³ Maxwell,⁴ and Olsen-Bär.⁵

2. MEASUREMENTS ON TIN

(a) Samples

The two samples of tin metal which had isotope distributions differing from the distribution occurring in nature were obtained from the AEC.⁶ The natural metal ($M=118.7$) was obtained from the Johnson, Matthey Company. The purities of the samples are listed in Table I.

The metal was cast under vacuum into thin-walled glass capillary tubes. The tin samples were about 0.8 mm in diameter and about 4 cm long. The wall thickness of the capillary tubing was about 0.2 mm.

(b) Experimental Results

The techniques used to determine the critical magnetic fields as a function of temperature were identical with those described in I. In addition to the two isotope samples, measurements were made on two samples of natural tin. The results for these two samples were the

³ Lock, Pippard, and Shoenberg, *Proc. Cambridge Phil. Soc.* **47**, 811 (1951).

⁴ E. Maxwell, *Proceedings of the International Conference on Low Temperature Physics* (Oxford, England, August 22 to 28, 1951).

⁵ M. Olsen-Bär, *Nature* **168**, 245 (1951).

⁶ The isotopes were produced by Carbide and Chemical Division, Oak Ridge National Laboratory, Y-12 Area, Oak Ridge, Tennessee, and were obtained on allocation.